Electronic Supplementary Information

Ultrasensitive homogeneous detection of microRNAs in a single cell with specifically designed exponential amplification

Kejian Gao, Pengbo Zhang, Hui Wang, Honghong Wang, Fengxia Su and Zhengping Li *

Beijing Key Laboratory for Bioengineering and Sensing Technology, School of Chemistry and Biological Engineering, University of Science and Technology Beijing, 30 Xueyuan Road, Haidian District, Beijing 100083 P. R. China.

*Corresponding Author: lzpbd@ustb.edu.cn (Z. Li)

List of Contents:

1. Experimental section

Materials and apparatus. Bst DNA polymerase large fragment, ProtoScript II reverse transcriptase, Phusion HotStart Flex DNA polymerase and Vent (exo-) DNA polymerase were purchased from New England BioLabs (U.S.A.). HPLC-purified miRNAs, PAGE-purified DNA oligonucleotides, Recombinant RNase Inhibitor (RRI), Taq DNA polymerase, RNase-free water, dNTPs, 20 bp DNA ladder marker and 6 × nucleic acid sample loading buffer were obtained from Takara Biotechnology Co., Ltd. (Dalian, China). The sequences of miRNAs and DNA oligonucleotides used in this work were listed in Table S1 and Table S2. SYBR Green I (20 ng/μL stock solution in DMSO) was purchased from Xiamen Bio-Vision Biotechnology Co. Ltd. (Xiamen, China). The betaine was obtained from Sigma (U.S.A.). The commercial Stem-loop RT-PCR Kit was ordered from Life Technology (Applied Biosystems, U.S.A.). 2720 Thermal Cycler (Bio-Rad, U.S.A.) was used to control the reaction temperature. The StepOne Real-Time PCR system (Applied Biosystems, U.S.A.) was employed for real-time fluorescence measurement.

Table S1. The sequence of miRNAs.

Name	Sequence (5'-3'direction)
let-7a	UGAGGUAGUAGGUUGUAUAGUU
let-7b	UGAGGUAGUAGGUUGUGUGGUU
let-7c	UGAGGUAGUAGGUUGUAUGGUU
let-7d	AGAGGUAGUAGGUUGCAUAGUU
let-7e	UGAGGUAGGAGGUUGUAUAGUU
let-7f	UGAGGUAGUAGAUUGUAUAGUU
let-7g	UGAGGUAGUAGUUUGUACAGUU
let-7i	UGAGGUAGUAGUUUGUGCUGUU
miR-143	UGAGAUGAAGCACUGUAGCUC

Table S2. The sequence of the DNA primers used in this work.

Name	Sequence (5'-3' direction)
SLRT-let-7a	CGACAGCAGAGGATTTGTTGTGTGGAAGTGTGAGCGGATT TTCCTCTGCTGTCGTTTTTAACTATACAAC
SLE- let-7a	ATCGTCGTGACTGTTTGTAATAGGACAGAGCCCCGCACTTT CAGTCACGACGATTTTTTTGAGGTAGTAG
SLRT-miR-143	CGACAGCAGAGGATTTGTTGTGTGGAAGTGTGAGCGGATT TTCCTCTGCTGTCGTTTTTGAGCTACAGT
SLE-miR-143	ATCGTCGTGACTGTTTGTAATAGGACAGAGCCCCGCACTTT CAGTCACGACGATTTTTTTGAGATGAAGC
FIP	CGACAGCAGAGGATTTGTTGTGTGGAAGTGTGAGCGGA
BIP	ATCGTCGTGACTGTTTGTAATAGGACAGAGCCCCGCAC

Reverse transcription reaction. The reverse transcription reaction was performed in a 5 μL solution including 1 μL diluted miRNA or cell lysate and 4 μL reaction solution which contained 0.25 mM dNTPs, 10 nM SLRT, 4 U RRI, 20 U ProtoScript II reverse transcriptase, 50 mM Tris-HCl and 3 mM $MgCl_2$ (pH 8.3 @ 25 °C). After mixing thoroughly, the reaction solution was incubated at 37 °C for 30 min to generate cDNA of miRNA target, 95 °C for 5 min to inactivate ProtoScript II reverse transcriptase and finally held at 4 °C.

cDNA amplification reaction. A volume of 5 μL solution containing 10 nM SLE, 0.2 U Phusion Hot Start Flex DNA Polymerase, 1 × Phusion HF buffer was added into the solution from above reverse transcription reaction. After mixing, the final concentration of SLRT and SLE kept the same as 5 nM. The reaction mixture was incubated at 98 °C for 30 s, followed by 15 cycles of 98 °C for 15 s, 37 °C for 40 s and 72 °C for 20 s, and finally held at 4 °C.

LAMP reaction. A volume of 1 μL products mentioned above was added to LAMP reaction mixture containing 0.6 μM forward inner primer (FIP), 0.6 μM backward inner primer (BIP), 1 M betaine, 0.25 mM dNTPs, 0.4 ng/μL SYBR Green I, 1 × ThermoPol reaction buffer (20 mM Tris-HCl, 10 mM KCl, 10 mM $(NH_4)_2SO_4$, 2 mM $MgSO_4$, 0.1% Triton X-100, pH 8.8 @ 25 °C) and 2.4 U Bst DNA polymerase large fragment with a final volume of 10 μL. The mixture was immediately put into the StepOne Real-Time PCR system to perform LAMP reaction at 65 °C. The real-time fluorescence intensity was simultaneously monitored at intervals of 60 s.

Cell culture. MCF-7, HeLa, K562, A549, and MRC-5 cell lines were purchased from the cell bank of Chinese Academy of Science (Shanghai, China). The HeLa, MCF-7, K562, and MRC-5 cell lines were cultured in DMEM Medium (GBICO) containing 10% (v/v) fetal calf serum (GBICO), 1% $NaHCO_3$, 100 U/mL penicillin, 100 μg/mL streptomycin and 3 mM L-glutamine. The A549 cell line was cultured in F12K Medium (Sigma) containing 10% (v/v) fetal calf serum, 1% $NaHCO_3$, 100 U/mL penicillin, 100 μg/mL streptomycin and 3 mM L-glutamine. All of the cell lines were maintained at 37 °C under a humidified atmosphere containing 5% CO_2.

Cell collection. The cell lines were centrifuged at 700 rpm for 5 min to remove the culture medium after trypsinization (0.2% trypsin, 1 mM EDTA, Invitrogen), washed three times with cold D-PBS buffer, and then resuspended in cold D-PBS buffer at a concentration of ~100 cells/μL. The cells were counted with the help of a Narishige

micromanipulator system equipped on an Olympus IX53 inverted microscope with a monitor and individual cell can be captured and collected in individual PCR tube.

MiRNA detection in a single cell lysate. For the single-cell analysis, the caught single cell was lysed by heating 95 °C for 5 min to release miRNA from the cell, which was immediately transferred to the reverse transcription reaction. The subsequent procedures were conducted following essentially the same procedures stated above.

2. Schematic illustration of the recycling amplification mechanism of the LAMP reaction

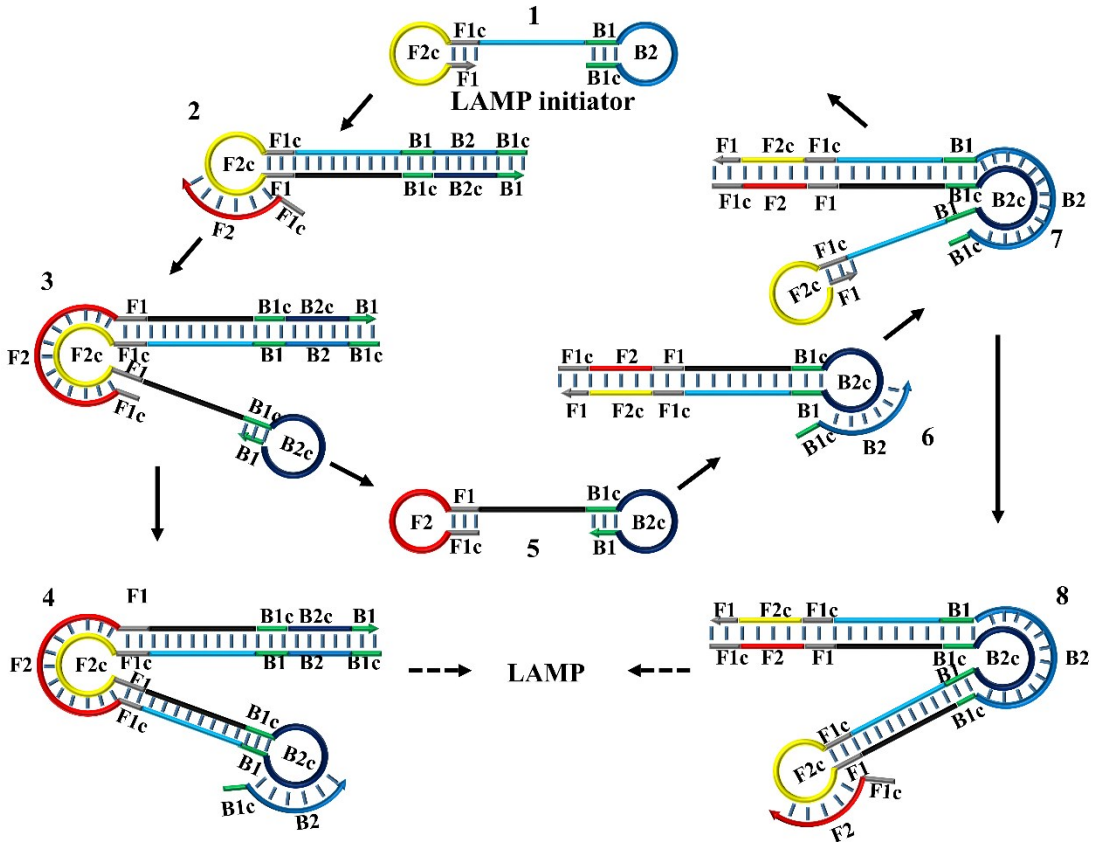

Fig. S1 Illustration of the recycling amplification mechanism of the LAMP reaction.

As descripted in Fig. S1, the double stem-loop DNA (structure 1) quickly converts to a stem-loop DNA (structure 2) by self-primed DNA synthesis at its 3'-terminus. Then, FIP hybridizes to the F2c sequence in the loop of the structure 2 and primes the extension reaction along the upper strand in the dsDNA. The dsDNA in structure 2 will be opened and the lower strand can be replaced to form a stem-loop DNA at its 3'-

terminus (structure 3). The self-primed extension of structure 3 will occur to generate a stem-loop structure with a longer stem-loop DNA (structure 4) and another double stem-loop DNA (structure 5). Structure 5 then generates structure 6 by self-primed DNA synthesis at its 3'-terminus. BIP then hybridizes to the B2c sequences in the loop of the structure 6 and extends to produce structure 7. The self-primed extension of structure 7 will further form another longer stem-loop DNA (structure 8) and release the starting material (structure 1) again, which means that the cycle reaction between structure 5 and structure 1 is established. In addition, both structure 4 and structure 8 can also act as the amplification templates to produce single and double stem-loop structure DNA with longer stems. The newly formed double stem-loop DNA will consecutively form new cycles of amplification. Therefore, rapid exponential amplification can be established to produce a large number of stem-loop DNA with various length of stems.

3. Validation of the amplification products using polyacrylamide gel electrophoresis (PAGE)

To further support the amplification mechanism of the proposed miRNA assay, the amplification products of LAMP reaction are characterized by non-denaturing PAGE. As shown in Fig. S2, the let-7a miRNA shows a defined band corresponding to 22 bp (lane 2). The products of reverse transcription reaction show a clear band in the presence of let-7a miRNA target (lane 4), indicating that the SLRT is reversely transcribed to form cDNA. After 15 cycles' amplification, a clear band exists at the position of 140 bp (lane 7), demonstrating the formation of the double stem-loop DNA which is the starting material of LAMP and can undergo the subsequent LAMP spontaneously. According to the principle in Fig. S1, the final amplification products are composed of a large amount of stem-loop DNA with various lengths. As shown in lane 8, the ladder-like patterns of bands are well consistent with the prediction from the proposed assay. By contrast, the blank control without let-7a miRNA does not produce any observable band of amplification products except for the unreacted FIP and BIP (lane 9). These results demonstrate that one miRNA molecule can generate a large amount of double stem-loop DNA through the amplification procedure similar to PCR and each double stem-loop DNA can initiate one LAMP reaction, resulting in the

ladder-like patterns of final amplification products.

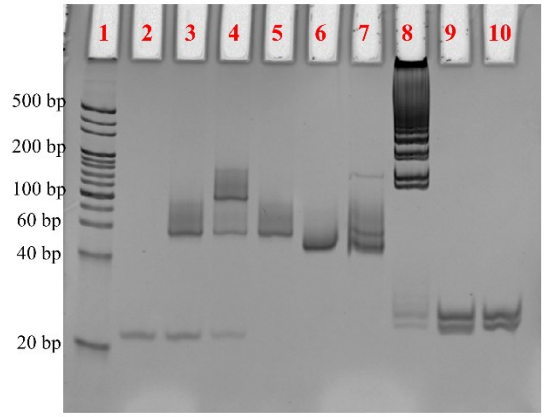

Fig. S2 Electrophoregram of non-denaturing PAGE analysis. Lane 1: double strand (ds) DNA markers (20 bp DNA ladder); lane 2: let-7a miRNA (500 nM); lane 3: SLRT + let-7a miRNA (each of 500 nM); lane 4: RT product; lane 5: SLRT (500 nM); lane 6: SLE (500 nM); lane 7: cDNA amplification product; lane 8: final amplification product in the presence of 100 pM let-7a miRNA; lane 9: final amplification product of blank; lane 10: FIP+BIP (500 nM).

4. The effect of the concentration of SLRT and SLE on the proposed miRNA assay

The concentration of the SLRT and SLE is a critical factor to affect the formation of the double stem-loop structure which is the essential element for the LAMP reaction. The concentration of SLRT and SLE is optimized with the range from 500 pM to 50 nM. As shown in Fig. S3, when the concentration of SLRT and SLE is 500 pM, the fluorescence signal produced by 1 fM let-7a miRNA cannot be observed within 60 min. The reason may be that lower concentration of SLRT and SLE generates less amount of double stem-loop structure DNA, which leads to the relatively low efficiency of LAMP reaction particularly at the lower concentration of target miRNA. By increasing the concentration of SLRT and SLE to 5 nM, the amplification reaction is accelerated and 10 aM let-7a miRNA target can be clearly detected. In addition, the fluorescence signal produced by the blank maintains to be a straight line within 60 min, indicating the near-zero non-specific amplification in the proposed miRNA assay. However, when the dosage of SLRT and SLE is further increased to 50 nM, the blank signal is greatly enhanced as depicted in Fig. S3c, which indicates that excessive SLRT and SLE may

cause much target-independent nonspecific amplification. Therefore, 5 nM of SLRT and SLE is employed for the miRNA assay in this work.

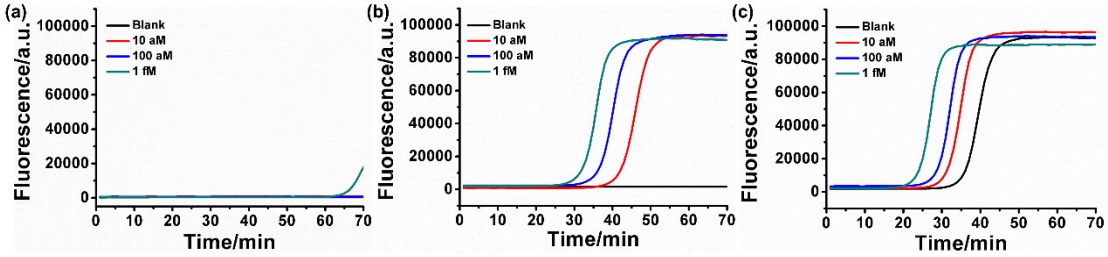

Fig. S3 The effect of concentration of SLRT and SLE on the detection of miRNA. The real-time fluorescence curves are produced by 0 (blank), 10 aM, 100 aM and 1 fM let-7a miRNA. The concentration of the SLRT and SLE is (a) 500 pM, (b) 5 nM and (c) 50 nM, respectively. Other experimental conditions are the same as described in the experimental procedure.

5. Optimization of thermal cycle number in the cDNA amplification

The sensitivity of the assay depends on the amplification efficiency and non-specific amplification derived from primer-dimers of SLRT and SLE during the thermal cycles, which is closely related to the number of thermal cycle in cDNA amplification. So the effect of the thermal cycle number during the cDNA amplification is investigated. As shown in Fig. S4, LAMP reaction gradually accelerates with increased thermal cycle number from 5 cycles to 20 cycles. With 5 cycle numbers, lower efficiency of cDNA amplification leads to smaller amount of double stem-loop DNA, resulting in lower sensitivity after LAMP reaction. As the number of thermal cycles increased to 15 cycles, well-defined exponential fluorescence curves ranging from 10 aM to 1 fM can be obtained and the fluorescence signals produced by blank keep at a very low level within the reaction time of 70 min, indicating that the sensitivity of the assay improved along with increased thermal cycle number. The amount of primer-dimers of SLRT and SLE is very little before 15 thermal cycles. Further increasing the thermal cycle number to 20, the blank generates detectable fluorescence signals due to the exponentially amplified primer-dimers with the increased thermal cycles. Therefore, in order to get the most accurate results, 15 cycles in the cDNA amplification is selected to be the optimum cycle number for the assay.

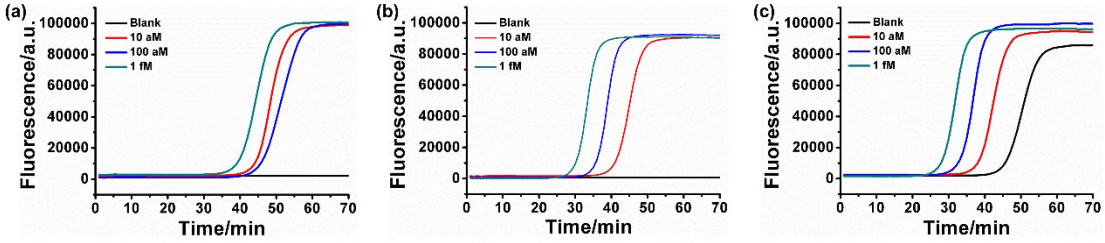

Fig. S4 The effect of thermal cycle number in the cDNA amplification of the proposed miRNA assay. The real-time fluorescence curves are produced by 0 (blank control), 10 aM, 100 aM and 1 fM let-7a miRNA. The thermal cycle number in the cDNA amplification is (a) 5 cycles, (b) 10 cycles and (c) 15 cycles, respectively. Other experimental conditions are the same as described in the experimental procedure.

6. The effect of different DNA polymerases on the miRNA assay

The efficiency of cDNA amplification during thermal cycles is an important factor influencing the sensitivity of the assay, therefore Phusion HotStart Flex DNA polymerase, Vent (exo-) DNA polymerase and Taq DNA polymerase are investigated in the proposed miRNA assay. As shown in Fig. S5b and c, the blank generated detectable fluorescence signal during LAMP reaction, which cannot be distinguished from the signal produced by 1 aM miRNA. The blank signals should result from the non-specific amplification derived from primer-dimers of SLRT and SLE during the thermal cycles. By contrast, the blank signal produced by Phusion HotStart Flex DNA polymerase is a straight line, which can be easily distinguished from the signals produced by 1 aM miRNA. The near-zero non-specific amplification may due to the nature of high fidelity of Phusion HotStart Flex DNA polymerase, which can decrease the occurrence of primer-dimers of SLRT and SLE during thermal cycles. Hence, the high-fidelity Phusion HotStart Flex DNA polymerase presents the best performance and is the most suitable DNA polymerase for our assay.

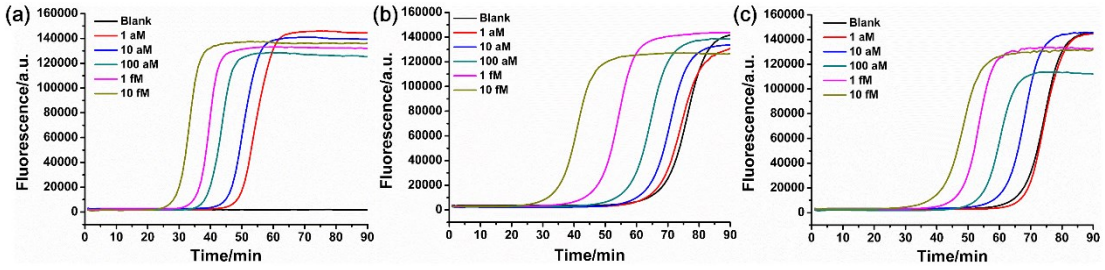

Fig. S5 The influence of DNA polymerase on the detection of miRNA using the proposed assay. The real-time fluorescence curves are produced by 0 (blank control), 1 aM, 10 aM, 100 aM, 1 fM and 10 fM let-7a miRNA using (a) Phusion HotStart Flex DNA polymerase, (b) Vent (exo-) DNA polymerase, and (c) Taq DNA polymerase as the DNA polymerase during thermal cycles, respectively. Other experimental conditions are the same as described in the experimental procedure.

7. Optimization of the amount of Phusion HotStart Flex DNA Polymerase

Due to the crucial effect on amplification efficiency during cDNA amplification reaction, the amount of Phusion HotStart Flex DNA polymerase is optimized. As shown in Fig. S6, as the amount of Phusion HotStart Flex DNA polymerase increased from 0.01 U/μL to 0.04 U/μL, the difference of point of inflection (POI) value between 100 aM and 1 fM let-7a miRNA first increases and then decreases, and reaches its maximum when the amount is 0.02 U/μL. In this regard, 0.02 U/μL Phusion HotStart Flex DNA polymerase is selected as the optimal amount for the proposed miRNA assay.

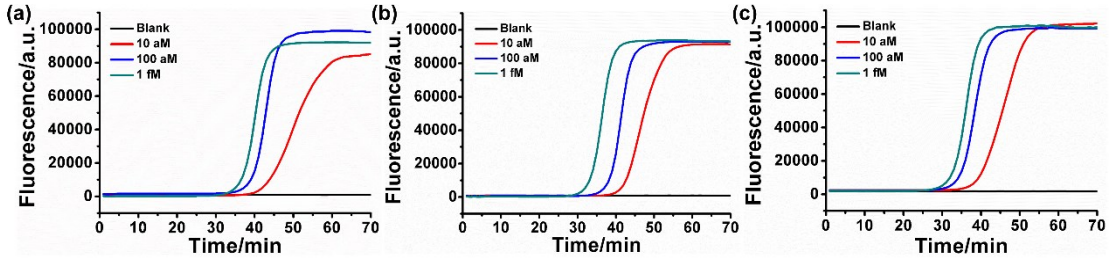

Fig. S6 The influence of the amount of Phusion HotStart Flex DNA polymerase on the proposed miRNA assay. The real-time fluorescence curves are produced by 0 (blank), 10 aM, 100 aM and 1 fM let-7a miRNA. The amount of Phusion HotStart Flex DNA polymerase used in the cDNA amplification reaction is (a) 0.01 U/μL, (b) 0.02 U/μL and (c) 0.04 U/μL, respectively. Other experimental conditions are the same as described in the experimental procedure.

8. Optimization of the amount of Bst DNA Polymerase

LAMP reaction relies on the catalysis of DNA polymerase with displacement activity. So the amount of Bst DNA polymerase is an important parameter for the assay. The effect of Bst DNA polymerase with different concentrations ranging from 0.08 U/μL to 0.40 U/μL on the proposed assay is investigated. As depicted in Fig. S7, when 0.08 U/μL Bst DNA polymerase is employed, no fluorescence signal for exponential amplification can be observed within the reaction time of 60 min, indicating that the

amount of Bst DNA polymerase is insufficient to produce efficient DNA extension. By increasing the amount of Bst DNA polymerase from 0.24~0.40 U/μL, LAMP reaction is gradually accelerated. However, the difference of POI between 10 aM, 100 aM and 1 fM let-7a miRNA gradually decreases. Taking into consideration of both reaction time and detection sensitivity, 0.24 U/μL is chosen as the optimal amount of Bst DNA polymerase for the proposed miRNA assay.

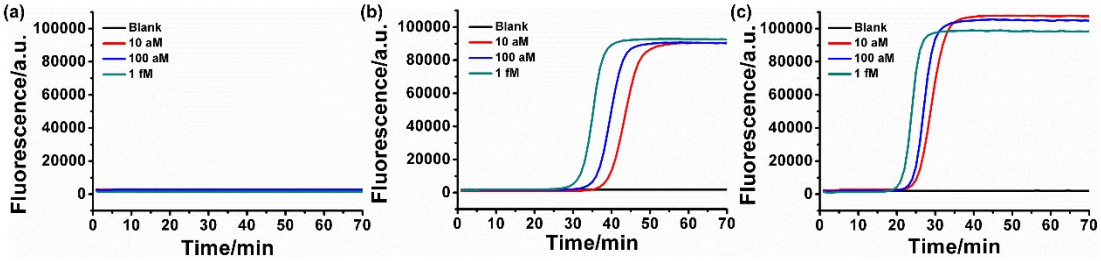

Fig. S7 The influence of the amount of Bst DNA polymerase on the proposed miRNA assay. The real-time fluorescence curves are produced by 0 (blank), 10 aM, 100 aM and 1 fM let-7a miRNA. The amount of Bst DNA polymerase used in the LAMP reaction is (a) 0.08 U/μL, (b) 0.24 U/μL and (c) 0.4 U/μL, respectively. Other experimental conditions are the same as described in the experimental procedure.

9. The amplification efficiency of the cDNA amplification reaction

In order to evaluate the amplification efficiency of the cDNA amplification reaction, the sensitivity of the assay in absence of cDNA amplification is assessed. The experimental conditions are the same as described in the experimental procedure except there is no thermal cycle. As depicted in Fig. S8, the fluorescence signal produced by 100 aM let-7a miRNA cannot be observed, demonstrating that the proposed assay without cDNA amplification of 15 thermal cycles can only detect let-7a miRNA greater than 1 fM. Compared with the result shown in Fig. 2a, the sensitivity can be increased 1000 times by adding 15 thermal cycles amplification during cDNA amplification, in which can detect as low as 1 aM miRNA. That is to say that the 15 thermal cycles can amplify the cDNA about 1000-fold.

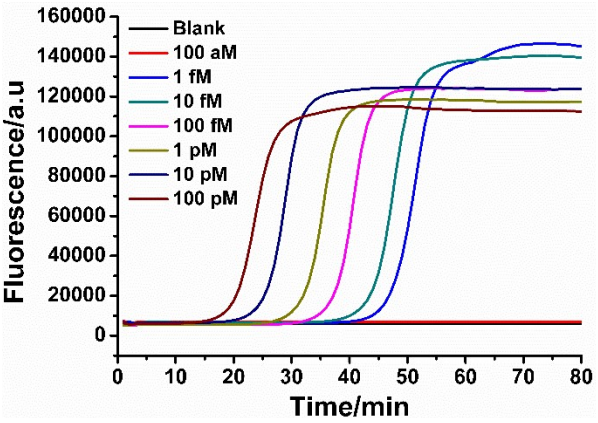

Fig. S8 Real-time fluorescence curves for the detection of let-7a miRNA by the proposed assay without cDNA amplification. From right to left, the concentration of let-7a miRNA is 0 (blank control), 100 aM, 1 fM, 10 fM, 100 fM, 1 pM, 10 pM and 100 pM, respectively. The blank was treated with the same procedures but without adding let-7a miRNA.

10. Evaluation of the universality and specificity of the proposed miRNA assay

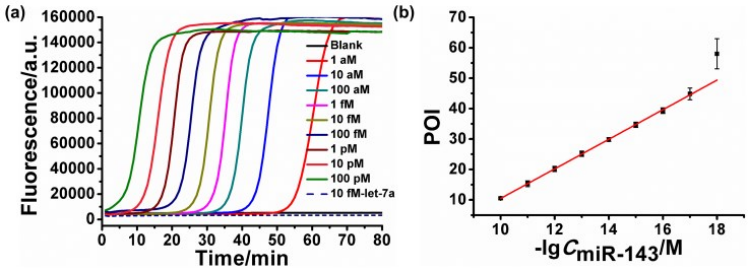

Fig. S9 Evaluation of the universality and specificity of the proposed miRNA assay. (a) Real-time fluorescence curves produced by different concentrations of miR-143 from 1 aM to 100 pM together with 10 fM let-7a miRNA (dashed line) by using the miR-143 sequence-specific SLRT and SLE. The blank was treated in the same way without miRNA target. (b) The linear relationship between POI value of the real-time fluorescence curve and logarithm of miR-143 concentration. The error bar was estimated from triplicate measurements.

11. Estimation of the interference of other let-7 miRNA members for let-7a miRNA detection

From the results of Fig. 2, the correlation equation for the determination of let-7a miRNA is POI=-31.74 − 4.47lg$C_{\text{let-7a}}$/M. As displayed in Fig. S10, the real-time fluorescence signal produced by let-7a miRNA could be obviously separated from those produced by any other let-7 family miRNA with the let-7a-specific SLRT and SLE primers. The POI values of let-7 family members could be obtained from the corresponding real-time fluorescence curves, which are supposed as POI_a, POI_b, POI_c, POI_d, POI_e, POI_f, POI_g and POI_i, respectively. On the basis of the correlation equation in Fig. 2, we presume that the POI_a, POI_b, POI_c, POI_d, POI_e, POI_f, POI_g and POI_i

corresponding to the amount of let- 7a are recorded as A_a, A_b, A_c, A_d, A_e, A_f, A_g and A_i, respectively. If the detection value of the let-7a (A_a) is normalized to be 100%, the relative detection value of other miRNA ($A_{other\ miRNA}/A_a$) can be calculated respectively.

According to the above-mentioned correlation equation, the following equation could be gained.

$$POI_b - POI_a = -4.47\ (\lg A_b - \lg A_a) \quad (1)$$

$$\lg \frac{A_b}{A_a} = -\frac{POI_b - POI_a}{4.47} \quad (2)$$

From Fig. S10a, the POI_a, POI_b, POI_c, POI_d, POI_e, and POI_f *are 3*0, 34, 33, 41, 43 and 37, respectively. As a consequence, $\frac{A_b}{A_a}$ could be calculated as 12.7% through the above constructed equations. According to the same process, $\frac{A_c}{A_a}$, $\frac{A_d}{A_a}$, $\frac{A_e}{A_a}$, and $\frac{A_f}{A_a}$ can be calculated as 23.6%, 1.0%, 0.4% and 4.6%, respectively. Therefore, the interference for the detection of let-7a miRNA arisen from the signals produced by let-7b, c, d, e and f was estimated to be 12.7%, 23.6%, 1.0%, 0.4% and 4.6%, respectively. Moreover, the signals produced by let-7g and let-7i are straight lines, indicating that they don't interfere with the detection of let-7a miRNA.

In consideration of the only one nucleotide difference near the 3'-terminus between let-7a and let-7c (base A in let-7a and base G in let-7c) and the similar binding energy between A:T and G:T, let-7c produces maximum nonspecific signal of 23.6%. Although two nucleotides difference exists compared with let-7a, let-7b still produces 12.7% nonspecific signal because of the mismatch site is near the 3'-terminus. In contrast, let-7e with the mismatched nucleotide close to the extension site of SLE (the 3'-terminus of SLE) produces 0.4% nonspecific signal. The mismatched nucleotide of let-7f just locates at the extension site of SLRT (the 3'-terminus of SLRT), resulted in a 4.6% nonspecific signal. Other let-7 miRNA family members (let-7d, let-7g and let-7i) and miR-143 produce negligible nonspecific signals (less than 1.0%). Therefore, the proposed assay can differentiate a single nucleotide difference with high specificity.

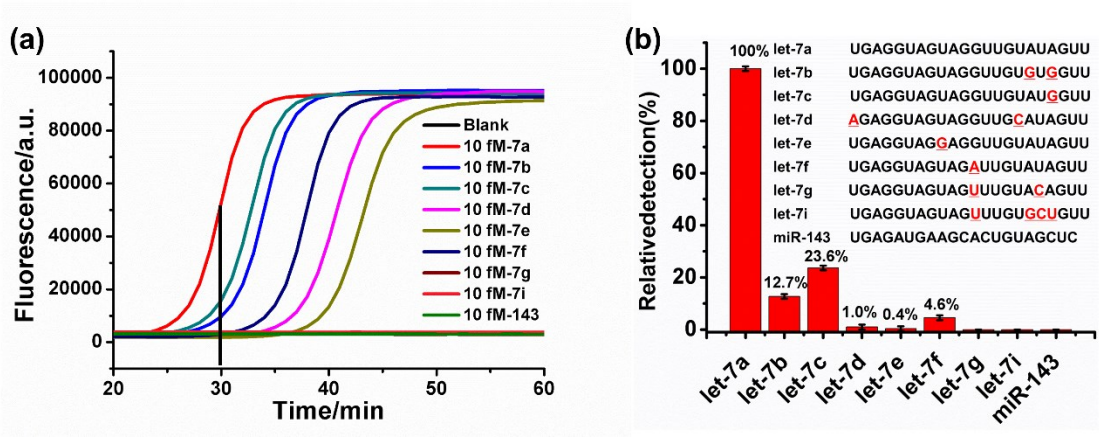

Fig. S10 Evaluation of the specificity for miRNA detection. The relation detection of the let-7a was normalized to 100%, and the relation detection of other miRNAs was calculated by the correlation equation from Fig. 2b. The concentration of each miRNA was 10 fM. The inset was the sequence list of let-7 miRNA family members and the different nucleotides of other let-7a family members compared with let-7a were marked in red. The error bar was estimated from triplicate measurements.

12. Quantification of miRNA in real biological samples with the proposed assay

With the proposed assay, the amount of let-7a miRNA in the total RNA sample extracted from MCF-7 is detected according to the standard experiment procedure described in the experimental section expect that let-7a miRNA is replaced by the total RNA sample. As illustrated in Fig. S11, the amount of MCF-7 total RNA samples ranging from 1 pg to 1 ng can be accurately detected by the proposed assay. There is a good linear relationship between the POI value and the logarithm (lg) of the different amount of total RNA. The correlation equation is POI=-10.28 − 4.79*lg*(total RNA input/g) with the corresponding correlation coefficient R^2 of 0.992. Therefore, as low as 1 pg total RNA can be clearly determined with our proposed assay, suggesting that our method has the ability to detect miRNA in real biological sample with high sensitivity.

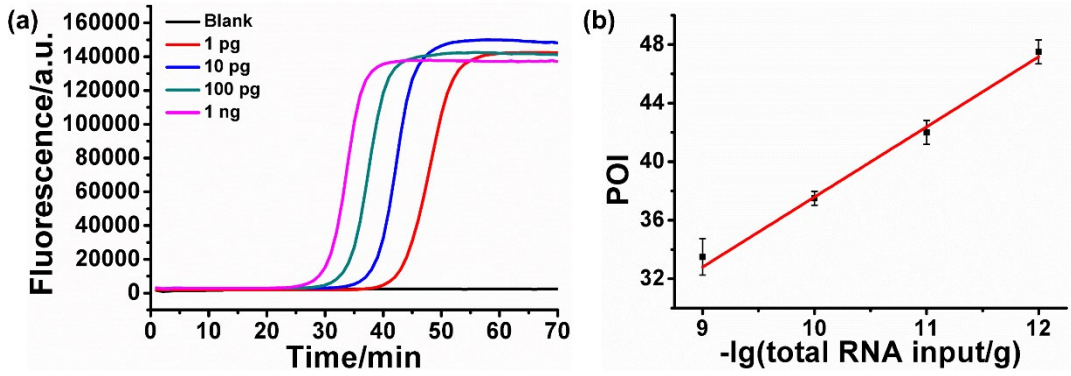

Fig. S11 The detection of miRNA in total RNA samples. (a) Real-time fluorescence curves produced by different amounts of total RNA (1 pg~1 ng). (b) The relationship between POI value

and the logarithm of the different amounts of total RNA. Error bars are calculated from three replicate measurements.

13. Quantification of miRNA in real biological samples using commercial stem-loop RT-PCR kit

To further verify the accuracy of the proposed method, the quantification of let-7a miRNA in the same batch of total RNA sample is evaluated using a commercial stem-loop RT-PCR kit. As shown in Fig. S12, the calibration curve between C_T value and the logarithm of target miRNA concentration in the range of 100 aM to 100 pM is obtained through serial dilutions of synthetic miRNA according to the protocol provided by the supplier. Therefore, we can calculate the concentration of let-7a miRNA in the total RNA sample according to the calibration curve. The concentration of let-7a miRNA in 10 pg total RNA extracted from MCF-7 is calculated to be 2.20 fM, which is consistent with the concentration originated from our proposed method (2.40 fM), indicating that the accuracy of our method is comparable to the commercial miRNA detection kit. These results demonstrate that the proposed assay is reliable and accurate for miRNA detection in real biological sample.

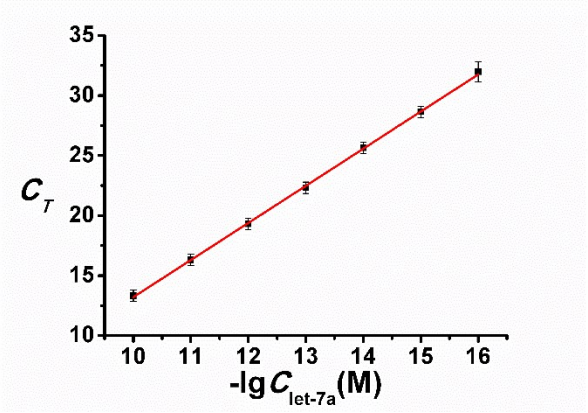

Fig. S12 The relationship between C_T value and the logarithm of the concentration of standard let-7a miRNA by stem-loop RT-PCR.

14. Detection of let-7a miRNA in individual cell lysate from MCF-7, K562, A549 and MRC-5 cell lines

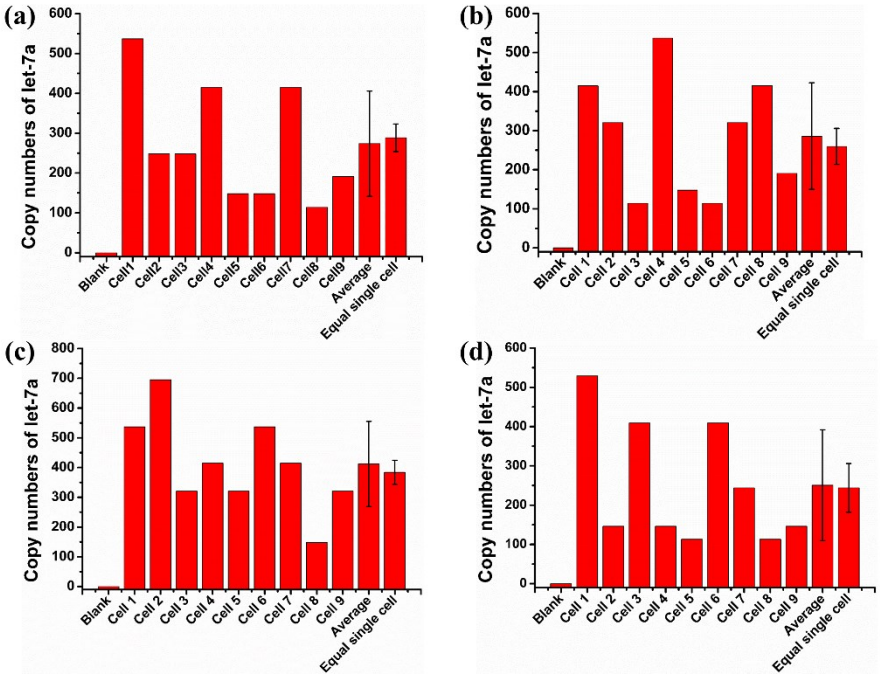

Fig. S13 Detection of let-7a miRNA from the 9 individual cell lysate of four types of cell lines by the proposed miRNA assay. (a) MCF-7, (b) MRC-5; (c) K562, and (d) A549.